Resonant generation of an Alfvén wave by a substorm injected electron cloud: a Van Allen probe case study

Olga S. Mikhailova[1], **Ekaterina E. Smotrova**[1], **Pavel N. Mager**[1]

[1]Institute of Solar-Terrestrial Physics SB RAS, Irkutsk, Russia

Key Points:

- The resonant generation of an Alfvén wave by energetic electrons is observed.
- The observed wave is the fundamental harmonic, propagating eastward with azimuthal wave number of about 110–115.
- The wave was generated through the gradient instability and interacted with electrons via the drift resonance.

Corresponding author: Olga S. Mikhailova, `o_mikhailova@iszf.irk.ru`

Abstract

In the paper a unique phenomenon – the resonant generation of ultra-low frequency (ULF) wave by energetic electrons in the magnetosphere – is presented. On 27 October 2012 in the morning side of the magnetosphere Van Allen Probe A registered an ULF wave with period of 100 s and an amplitude of 0.7 nT. A cloud of energetic electrons was observed simultaneously with the wave. It is established that the electron cloud was injected into the magnetosphere as a result of a substorm. Electron fluxes in several energy channels were modulated with the frequency of the observed wave. It is shown that these flux modulations are caused by the drift resonance of 38 keV electrons and the wave being a fundamental harmonic of an Alfvén mode with an azimuthal wavenumber $m \sim 110$–115 propagating to the east, and generated through the gradient instability due to steep earthward density gradient of the resonant electrons.

Plain Language Summary

In recent decades, with the increase in the number of magnetospheric missions, information about wave phenomena has been significantly replenished. Most of ultra-low frequency (ULF) waves observed by satellites interact with high-energy protons, and there is very little evidence of resonant interaction with electrons. Using observations of the Van Allen Probe A, we found a unique phenomenon of resonant generation of ULF wave by energetic electrons injected into magnetosphere during the substorm onset. We established that the found Alfvén wave was generated through instability caused by the strong radial inhomogeneity of density of 38 keV electrons being in the drift resonance with the wave (the drift velocity of the electrons coincides with the phase velocity of the wave).

1 Introduction

Ultra-low frequency (ULF) waves are regularly observed in the Earth's magnetosphere. They are a convenient magnetospheric diagnosing tool because they are able to interact with energetic charged particles. ULF waves of the Pc4–5 (40–600c) ranges most often are Alfvén waves standing along the magnetic field line between magnetically conjugated points of the ionosphere. Besides, the observed Alfvén waves differ in polarization (Anderson et al., 1990): if the radial component of the wave's magnetic field is much larger than the azimuthal component, then such a wave is called a poloidal Alfvén wave, and in the opposite case a wave is called a toroidal one. Poloidal Alfvén waves can interact with charged particles via the drift or drift-bounce resonances (Klimushkin et al., 2021), since they have significant azimuthal component of the wave electric field coinciding with particle drift direction, which leads to acceleration or deceleration of them. These resonant interactions are important for the dynamics of the ring current (Southwood et al., 1969) and radiation belt (Schulz & Lanzerotti, 1974) particles. Moreover, through these types of resonances poloidal Alfvén waves can be generated by two types of instability. First, gradient instability caused by a steep earthward particle density gradient at a resonant energy. Second, the bump-on-tail instability, when a velocity distribution of the particles is inverted around the resonant energy, that is there is a bump at the energetic part of the distribution (Southwood, 1976; Karpman et al., 1977; Chen & Hasegawa, 1988).

Most of the observed poloidal waves are the second harmonic of the Alfvén wave. They are asymmetric in the electric field relative to the equator and are generated by the drift-bounce resonance (Southwood et al., 1969; Hughes et al., 1978; Takahashi et al., 1990; Chen & Hasegawa, 1994; Min et al., 2017; Takahashi, Oimatsu, et al., 2018; Rubtsov et al., 2021). It should be noted, that the drift-bounce resonance is impossible with energetic electrons, since due to their small mass the frequencies of their bouncing motion along field lines is much higher than the wave frequency. The fundamental (symmetric) harmonic of poloidal waves is less common and is generated as a result of the drift resonance (Dai et al., 2013; Mager et al., 2018; Takahashi, Claudepierre, et al., 2018). They are often identified as giant magnetic pulsations (Pg) observed on Earth (Glassmeier et al., 1999; Takahashi, Claudepierre, et al., 2018; Mager & Klimushkin, 2013).

In all the cases listed above, the resonant interactions of ULF waves with protons were studied. Interactions with electrons are observed much less frequently (Claudepierre et al., 2013; Ren et al., 2017, 2018, 2019; Hao et al., 2020), although it was shown in (Chelpanov et al., 2019; James et al., 2013) that up to 20% of the observed ULF waves can have positive azimuthal wavenumbers. In that case the directions of the wave propagation and the electron drift coincide, which implies the interaction of the wave with electrons via drift interaction. Although, the mentioned works investigated the electron-wave interaction, they were aimed to study the acceleration of cold electrons (Ren et al., 2017, 2018, 2019; Hao et al., 2020) and the mechanisms of the wave generating were not related to the electrons. Claudepierre et al. (2013) studied the interaction of the wave with energetic electrons. Several potential generation mechanisms for the observed ULF wave were proposed but they have not been investigated yet. In our paper, we present a study of an unique event —- the resonant generation of an Alfvén wave by substorm injected cloud of energetic electrons through the gradient instability.

2 Oscillations and Geomagnetic Conditions

Using the Van Allen Probes A data, the 27 October 2012 event was investigated. To study oscillations in a magnetic field, we used 4-second data from the Electric and Magnetic Field Instrument Suite and Integrated Science (EMFISIS) (Kletzing et al., 2013) and 11-second data from the Electric Fields and Waves (EFW) instrument (Wygant et al., 2013) to study oscillations in an electric field. Eleven-second data from the Magnetic Electron Ion Spectrometer (MagEIS) instrument were used to study electron fluxes (Blake et al., 2013). The satellite registered an ULF wave with a duration of 45 minutes and amplitude of about 0.7 nT and 3 mV in the magnetic and electric fields, respectively (Fig. 1). The wave frequency was 10 mHz (Pc4 range) and did not vary during the registration period. The wave had a mixed polarization: the poloidal (radial) b_r and toroidal (azimuthal) b_a components of the wave magnetic field are slightly different as well as the corresponding transverse electric field components. The parallel (compressional) magnetic component $b_{\|}$ is significantly weaker than the radial and azimuthal components. Therefore, we can conclude that the observed wave most likely was an Alfvén wave, rather then some kind of compressional mode.

We also calculated the values of the Alfvén eigenfrequencies of the poloidal and toroidal harmonics (FLR – field line resonances). Figure 1b shows the calculated Alfvén eigenfrequencies for cold plasma. In the calculations the dipole approximation for the background magnetic field is assumed. One can see a good agreement: the observed wave frequency falls into the range between the calculated poloidal (red line) and toroidal (yellow line) eigenfrequencies, which corresponds to the mixed polarization of the wave.

The event was registered in the morning side of the magnetosphere at a distance of about 6 R_E from the Earth (Fig. 2a). The ULF wave was observed outside the plasmasphere (Fig. 2b), in the region where the plasma density is of about 1 cm^{-3}. There were quiet geomagnetic conditions during the event: geomagnetic indices were Kp = 1, Dst = – 17 nT (World Data Center for Geomagnetism, Kyoto et al., 2015). Nevertheless several substorms preceded the event. About 70 minutes before the start of the event,

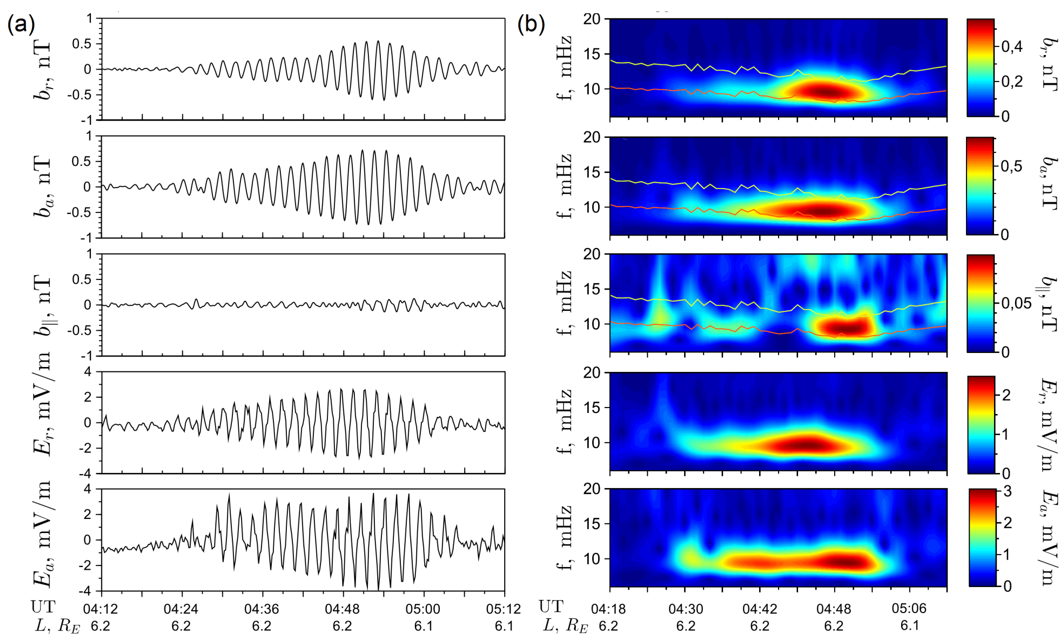

Figure 1. a) Oscillations in the magnetic and electric fields (from top to bottom: radial, azimuthal and parallel components of the magnetic field, radial and azimuthal components of the electric field). b) Wavelet spectra of corresponding oscillations. The lines mark the calculated Alfvén eigenfrequencies: the red line is the poloidal frequency of the fundamental harmonic, the yellow line is the toroidal one.

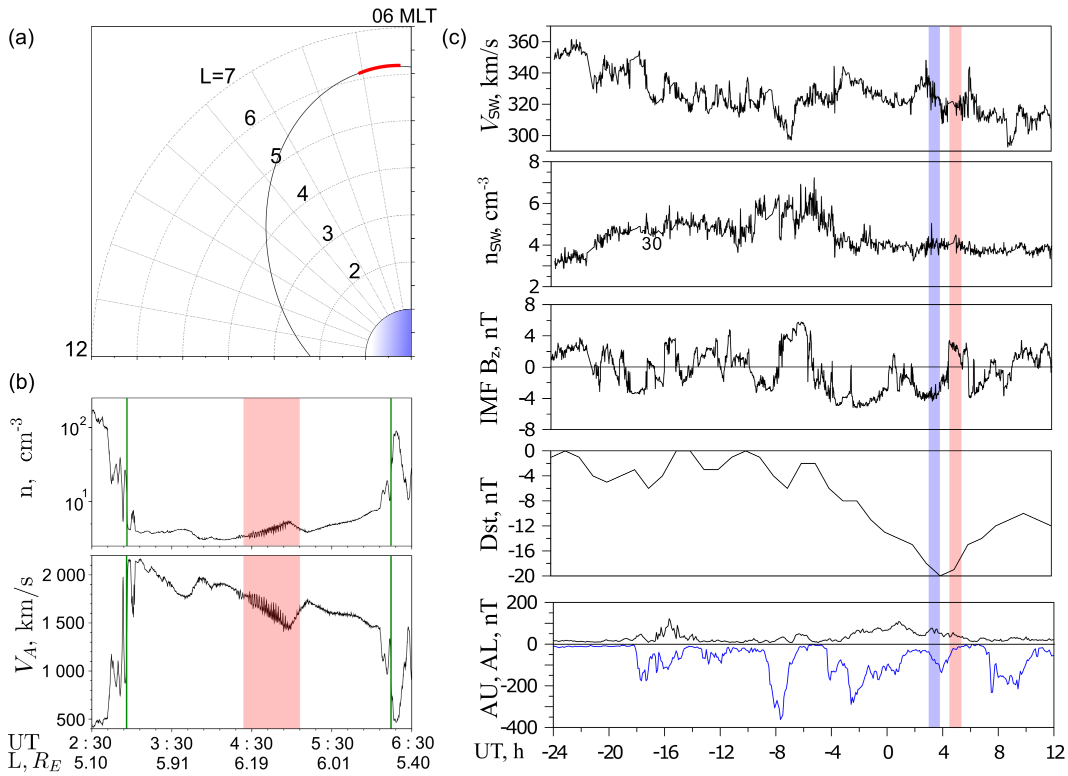

Figure 2. a) The trajectory of Van Allen Probe A on 27 October 2012 when the wave was observed (time of the wave event is marked with a red arc). b) The electron density and the Alfvén velocity. Red rectangles highlight the time of the wave event, the plasmapause is marked with green lines. c) Geomagnetic conditions from top to bottom: solar wind speed and density, z-component of the Interplanetary Magnetic Field (IMF), Dst index, AU and AL auroral electrojet indices. Here the time interval of the wave registration by Van Allen Probe A is highlighted with a red rectangle, and the time interval when Van Allen Probe B was passing the same region is highlighted with a blue rectangle.

the substorm was registered (onset time 03:14 UT) with minimum AL index value of about -150. Van Allen Probe B passed the region where the wave was observed an hour earlier. It did not record noticeable oscillations. As one can see from the AL index in Figure 2c, at this time (highlighted in blue) a substorm was developing. At the moment when satellite A crossed the region and registered the studied wave (highlighted in red), the main phase of the substorm had already passed and the recovery phase had started. Probably, this substorm was a source of energetic particles, that are ultimately responsible for generating the observed wave.

3 Modulations in the Electron Fluxes

Unfortunately, data for proton fluxes and data on cold electrons for the event time period are not availible. Despite this, we had access to electron data with energies from 38 keV to 2 MeV (data from the MAGEIS instrument). We were lucky to find modulations in electron fluxes at the several energy channels: 38, 58, and 82 keV. Fluxes are harmonically modulated with the wave's frequency during the period of the wave registration. The strongest modulations are seen at the energy 38 keV (Fig. 3a). It corresponds to the maximal spectral peak in the cross spectra of the azimuthal component of the electric field E_a and the relative electron flux oscillations $\delta J/J$ at the wave frequency 10 mHz (Fig. 3c). As seen from Fig. 3b the flux oscillations have the maximum amplitude for particles with pitch angles of 90° and are in phase at conjugate pitch angles. This pitch angle distribution of the modulated flux corresponds to the fundamental (the wave electric field is symmetric relative to the equator) harmonic of the Alfvén wave and the wave-particle drift resonance (Southwood, 1976; Southwood & Kivelson, 1982). In addition, we found that E_a is in phase with $\delta J/J$ at the energy of 38 keV. The phase shift $\Delta\phi$ is close to zero at 38 keV and grows with energy (Fig. 3d), which allows us to conclude that the resonant energy of the electrons is close to 38 keV. All facts mentioned above lead to a conclusion that the observed electron flux oscillations were caused by the drift resonance and that we observe the fundamental harmonic of the standing Alfvén wave.

The drift resonance condition can be written as

$$\omega - m\omega_d = 0, \tag{1}$$

where ω is the wave frequency, m is the azimuthal wave number, and ω_d is the angular velocity of the particle magnetic drift averaged over the bounce period. Using condition

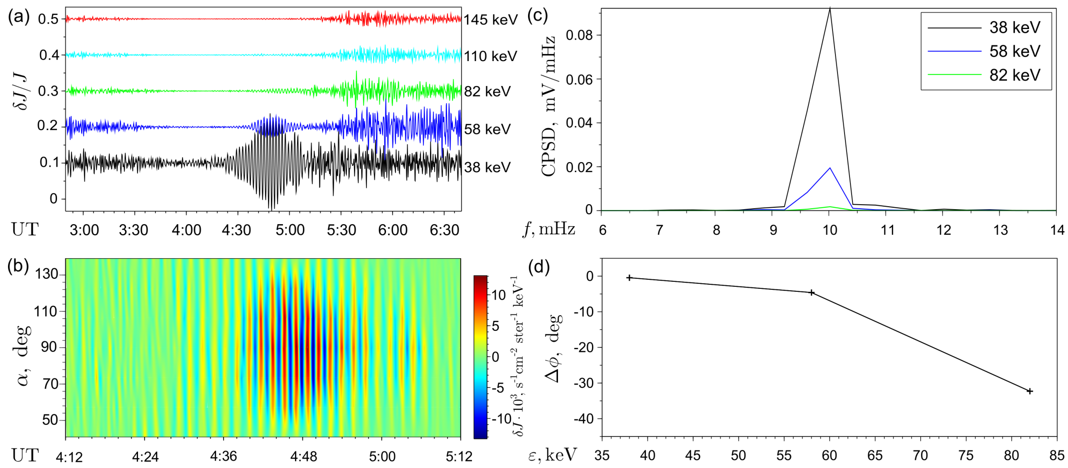

Figure 3. a) Relative electron flux oscillations ($\delta J/J$) for different energies, where δJ and J are perturbed and unperturbed fluxes, respectively, separated by filtration. b) Pitch angle distribution of δJ for 38 keV electrons. c) Cross power spectral density (CPSD) and d) cross-phase $\Delta\phi$ between E_a and $\delta J/J$ for 38, 58, and 82 keV.

(1), we calculated the azimuthal wave number $m \simeq$110–115. The corresponding azimuthal wavelength λ_a is approximately 2200 km, i.e. about 0.3 R_E. Thus, the wave was azimuthally small-scale and propagating eastward (from night to day) in the direction of the energetic electron drift. Since $\lambda_r/\lambda_a = |b_r/b_a|$ and $|b_r/b_a| \sim 1$, the radial wavelength λ_r is also of about 0.3 R_E.

4 Instability

Wave amplitude increase via wave-particle energy transfer requires either non-equilibrium particle distribution, such as inverted distribution (a distribution with "bump-on-tail")(Southwood, 1976; Karpman et al., 1977; Hughes et al., 1978), or (and) a spacial distribution with a steep earthward gradient at a resonant energy (Chen & Hasegawa, 1988, 1991; Dai et al., 2013). Plasma instability caused by these non-equilibrium distributions arises when the following condition is satisfied

$$\hat{Q}F = \left[\frac{\partial F}{\partial \varepsilon} + \frac{m}{\omega}\frac{c}{qB_{eq}L}\frac{\partial F}{\partial L}\right]_{\varepsilon_{res}} > 0. \qquad (2)$$

Here F is the velocity distribution function, ε is the particle energy, q is the particle charge, c is the speed of light, B_{eq} is the magnetic field at the geomagnetic equator, L is the McIlwain parameter used as the radial coordinate, and ε_{res} is the resonant energy. The most frequently observed instability generating poloidal Alfvén waves is the bump-on-tail instability caused by the inverted distribution, that is the instability is realized when the condition $\partial F/\partial \varepsilon > 0$ is satisfied. However, we found $\partial F/\partial \varepsilon < 0$ throughout time period when the wave was observed. This means that the wave probably was generated through the gradient instability caused by an earthward gradient of the distribution, that is the condition $\partial F/\partial L < 0$ must be satisfied. Indeed, such conditions are met between 04:00 UT and 04:50 UT. The radial gradient was negative and wherein the instability condition Eq. (2) was satisfied on two parts of the satellite trajectory: from 04:00 to 04:27 UT, when the satellite was moving away from the Earth, and from 04:27 to 04:50 UT, when the satellite was moving toward the Earth (Fig. 4a, b). Note that the radial gradient was calculated using one satellite under the assumption that the azimuthal motion of the satellite is small compared to radial one. Thus, the area where the wave was observed almost coincides with the area where the instability is realized.

We assume that the wave could have been generated as a result of electron injection into the magnetosphere during the substorm. Using the electron flux data, we were able to localize the onset of the substorm that provided the electron cloud. Using the idea that particles with different energies move with different angular velocities, $\omega_d \propto \varepsilon$, we calculated the time interval between the injection and the wave observation. We determined that the onset of the substorm occurred at 03:14 UT. This time corresponds to the time of the substorm beginning according to the AL index. In addition, we found that the substorm occurred at midnight on MLT. Figure 4c shows a schematic representation of the motion and transformation of a mono-energetic electron cloud from the onset location. Farther from the Earth electrons drift at a higher angular velocity than those closer to the Earth, since $\omega_d \propto L$. As a result, the cloud is stretched into a narrow stripe, leading to an increase in the radial gradient of the electron density. Thus, this mechanism creates the necessary conditions for the instability, which, as a result, leads to generation of ULF waves.

5 Conclusion

Using Van Allen Probe A data we were able to observe and study in detail a unique phenomenon of the resonant generation of the ULF wave by energetic electrons in the magnetosphere.

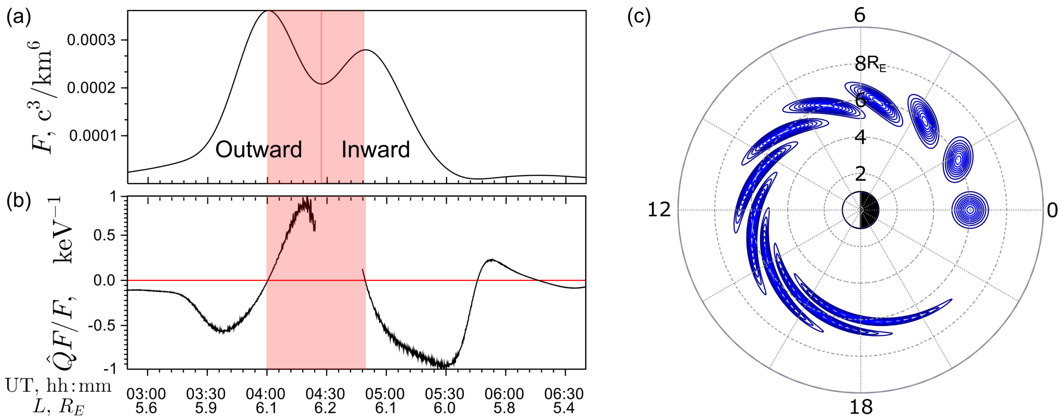

Figure 4. a) The electron distribution function against UT and L. The area of the negative radial gradient is highlighted in red: from 04:00 to 04:27 UT when the satellite is moving away from the Earth (outward) and from 04:27 to 04:50 UT when the satellite is moving towards the Earth (inward). The red line at 04:27 UT indicates the time of the apogee position. b) The instability condition from Eq. 2. The instability coefficient is positive from 04:00 to 04:50 UT, the area near the apogee of the satellite ($L = 6.2$) is excluded due to the uncertainty of the radial gradient. c) A schematic representation of the substorm injected electron cloud.

It is found, that the fundamental harmonic of the Alfvén wave with a period of about 100 s was observed in the morning sector of the magnetosphere at a distance of about 6 R_E from the Earth. The wave had almost equal amplitudes in the radial and azimuthal components of the magnetic and electric fields, that is the wave had a mixed polarization. Simultaneously with the wave, resonant oscillations were observed in several electron fluxes at energies from 38 to 82 keV. We show that electrons interact with the wave via the drift resonance. It is established that the resonant electrons had energy of about 38 keV. From the electron drift velocity and wave phase velocity equility condition for the drift resonance, we found the azimuthal wave number $m = 110$–115, which means that the wave was azimuthally small-scale and eastward propagating. It is shown that the wave was generated by the gradient instability caused by a steep earhward density gradient of the resonant electrons. It is determined that the cloud of the energetic electrons led to the wave generation was injected into the magnetosphere during a substorm.

Data Availability Statement

The Van Allen Probes data used in this paper are available at the CDAWeb site (https://cdaweb.gsfc.nasa.gov/pub/data/rbsp/rbspa/). The solar wind and IMF data, AU, AL, and Dst indices were obtained from the Goddard Space Flight Center Space Physics Data Facility OMNIWeb (https://spdf.gsfc.nasa.gov/pub/data/omni/).

Acknowledgments

The work of O.S.M. was financially supported by the Grant of the Russian Scientific Foundation (project No. 21-72-10139) in terms of modulations in electron fluxes and instability studying (Sections 1, 3, 4). The work of E.E.S. and P.N.M. was financially supported by Ministry of Science and Higher Education of the Russian Federation in terms of magnetic and electric fields data processing (Section 2) and the simulation of the electron cloud motion (Section 4). We acknowledge the NASA Van Allen Probes and Craig Kletzing for use of EMFISIS data, John Wygant for use of EFW data, Bern Blake for use of ECT/MagEIS data. The authors are thankful to Dmitri Yu. Klimushkin and to Maksim A. Chelpanov for valuable discussions.

References

Anderson, B. J., Engebretson, M. J., Rounds, S. P., Zanetti, L. J., & Potemra, T. A. (1990). A statistical study of Pc 3-5 pulsations observed by the AMPTE/CCE magnetic fields experiment. 1. Occurrence distributions. *Journal of Geophysical Research*, *95*, 10495-10523. doi: 10.1029/JA095iA07p10495

Blake, J. B., Carranza, P. A., Claudepierre, S. G., Clemmons, J. H., Crain, W. R., Dotan, Y., ... Zakrzewski, M. P. (2013, jun). The magnetic electron ion spectrometer (MagEIS) instruments aboard the radiation belt storm probes (RBSP) spacecraft. *Space Science Reviews*, *179*(1-4), 383–421. doi: 10.1007/s11214-013-9991-8

Chelpanov, M. A., Mager, P. N., Klimushkin, D. Y., & Mager, O. V. (2019). Observing magnetospheric waves propagating in the direction of electron drift with Ekaterinburg Decameter Coherent Radar. *Solar-Terrestrial Physics*, *5*, 51-57. doi: 10.12737/stp-51201907

Chen, L., & Hasegawa, A. (1988). On magnetospheric hydromagnetic waves excited by energetic ring-current particles. *Journal of Geophysical Research*, *93*(A8),

8763. doi: 10.1029/JA093iA08p08763

Chen, L., & Hasegawa, A. (1991). Kinetic theory of geomagnetic pulsations: 1. Internal excitations by energetic particles. *Journal of Geophysical Research*, *96*, 1503-1512. doi: 10.1029/90JA02346

Chen, L., & Hasegawa, A. (1994). Kinetic theory of geomagnetic pulsations: 2. Ion flux modulations by transverse waves. *Journal of Geophysical Research*, *99*, 179-182. doi: 10.1029/93JA02774

Claudepierre, S. G., Mann, I. R., Takahashi, K., Fennell, J. F., Hudson, M. K., Blake, J. B., ... Wygant, J. R. (2013). Van Allen Probes observation of localized drift resonance between poloidal mode ultra-low frequency waves and 60 keV electrons. *Geophysical Research Letters*, *40*, 4491-4497. doi: 10.1002/grl.50901

Dai, L., Takahashi, K., Wygant, J. R., Chen, L., Bonnell, J., Cattell, C. A., ... Spence, H. E. (2013). Excitation of poloidal standing Alfvén waves through drift resonance wave-particle interaction. *Geophysical Research Letters*, *40*, 4127–4132. doi: 10.1002/grl.50800

Glassmeier, K.-H., Buchert, S., Motschmann, U., Korth, A., & Pedersen, A. (1999). Concerning the generation of geomagnetic giant pulsations by drift-bounce resonance ring current instabilities. *Annales Geophysicae*, *17*, 338–350. doi: 10.1007/s00585-999-0338-4

Hao, Y. X., Zhao, X. X., Zong, Q.-G., Zhou, X.-Z., Rankin, R., Chen, X. R., ... Claudepierre, S. G. (2020, aug). Simultaneous observations of localized and global drift resonance. *Geophysical Research Letters*, *47*(17). doi: 10.1029/2020GL088019

Hughes, W. J., Southwood, D. J., Mauk, B., McPherron, R. L., & Barfield, J. N. (1978). Alfvén waves generated by an inverted plasma energy distribution. *Nature*, *275*, 43–45. doi: 10.1038/275043a0

James, M. K., Yeoman, T. K., Mager, P. N., & Klimushkin, D. Y. (2013). The spatio-temporal characteristics of ULF waves driven by substorm injected particles. *Journal of Geophysical Research: Space Physics*, *118*, 1737-1749. doi: 10.1002/jgra.50131

Karpman, V. I., Meerson, B. I., Mikhailovsky, A. B., & Pokhotelov, O. A. (1977). The effects of bounce resonances on wave growth rates in the magnetosphere.

Planetary and Space Science, *25*, 573–585. doi: 10.1016/0032-0633(77)90064-2

Kletzing, C. A., Kurth, W. S., Acuna, M., MacDowall, R. J., Torbert, R. B., Averkamp, T., … Tyler, J. (2013, jun). The electric and magnetic field instrument suite and integrated science (emfisis) on rbsp. *Space Science Reviews*, *179*(1-4), 127–181. doi: 10.1007/s11214-013-9993-6

Klimushkin, D., Mager, P., Chelpanov, M., & Kostarev, D. (2021, dec). Interaction between long-period ulf waves and charged particle in the magnetosphere: theory and observations (overview). *Solar-Terrestrial Physics*, *7*(4), 33–66. doi: 10.12737/stp-74202105

Mager, P. N., & Klimushkin, D. Y. (2013). Giant pulsations as modes of a transverse Alfvénic resonator on the plasmapause. *Earth Planet. Space*, *65*, 397-409. doi: 10.5047/eps.2012.10.002

Mager, P. N., Mikhailova, O. S., Mager, O. V., & Klimushkin, D. Y. (2018). Eigenmodes of the Transverse Alfvénic Resonator at the Plasmapause: A Van Allen Probes Case Study. *Geophysical Research Letters*, *45*, 10,796-10,804. doi: 10.1029/2018GL079596

Min, K., Takahashi, K., Ukhorskiy, A. Y., Manweiler, J. W., Spence, H. E., Singer, H. J., … Cohen, R. J. (2017). Second harmonic poloidal waves observed by Van Allen Probes in the dusk-midnight sector. *Journal of Geophysical Research: Space Physics*, *122*(3), 3013-3039. doi: 10.1002/2016JA023770

Ren, J., Zong, Q. G., Miyoshi, Y., Rankin, R., Spence, H. E., Funsten, H. O., … Kletzing, C. A. (2018). A Comparative Study of ULF Waves' Role in the Dynamics of Charged Particles in the Plasmasphere: Van Allen Probes Observation. *Journal of Geophysical Research: Space Physics*, *123*, 5334-5343. doi: 10.1029/2018JA025255

Ren, J., Zong, Q. G., Miyoshi, Y., Zhou, X. Z., Wang, Y. F., Rankin, R., … Kletzing, C. A. (2017). Low-Energy (<200 eV) Electron Acceleration by ULF Waves in the Plasmaspheric Boundary Layer: Van Allen Probes Observation. *Journal of Geophysical Research: Space Physics*, *122*, 9969-9982. doi: 10.1002/2017JA024316

Ren, J., Zong, Q. G., Zhou, X. Z., Spence, H. E., Funsten, H. O., Wygant, J. R., & Rankin, R. (2019). Cold Plasmaspheric Electrons Affected by ULF

Waves in the Inner Magnetosphere: A Van Allen Probes Statistical Study. *Journal of Geophysical Research: Space Physics*, *124*, 7954-7965. doi: 10.1029/2019JA027009

Rubtsov, A. V., Mikhailova, O. S., Mager, P. N., Klimushkin, D. Y., Ren, J., & Zong, Q.-G. (2021, nov). Multispacecraft observation of the presubstorm long-lasting poloidal ulf wave. *Geophysical Research Letters*, *48*(23). doi: 10.1029/2021GL096182

Schulz, M., & Lanzerotti, L. J. (1974). *Particle diffusion in the radiation belts.* Berlin, Heidelberg, New York: Springer-Verlag.

Southwood, D. J. (1976). A general approach to low-frequency instability in the ring current plasma. *Journal of Geophysical Research*, *81*, 3340–3348. doi: 10.1029/JA081i019p03340

Southwood, D. J., Dungey, J. W., & Etherington, R. J. (1969). Bounce resonant interactions between pulsations and trapped particles. *Planetary and Space Science*, *17*, 349-361. doi: 10.1016/0032-0633(69)90068-3

Southwood, D. J., & Kivelson, M. G. (1982). Charged particle behavior in low-frequency geomagnetic pulsations. 2. Graphical approach. *Journal of Geophysical Research*, *87*, 1707-1710. doi: 10.1029/JA087iA03p01707

Takahashi, K., Claudepierre, S. G., Rankin, R., Mann, I., & Smith, C. W. (2018). Van Allen Probes Observation of a Fundamental Poloidal Standing Alfvén Wave Event Related to Giant Pulsations. *Journal of Geophysical Research: Space Physics*, *123*, 4574–4593. doi: 10.1029/2017JA025139

Takahashi, K., McEntire, R. W., Lui, A. T. Y., & Potemra, T. A. (1990). Ion flux oscillations associated with a radially polarised transverse Pc5 magnetic pulsation. *Journal of Geophysical Research*, *95*, 3717-3731. doi: 10.1029/JA095iA04p03717

Takahashi, K., Oimatsu, S., Nosé, M., Min, K., Claudepierre, S. G., Chan, A., ... Kim, H. (2018). Van Allen Probes Observations of Second Harmonic Poloidal Standing Alfvén Waves. *Journal of Geophysical Research: Space Physics*, *123*, 611-637. doi: 10.1002/2017JA024869

World Data Center for Geomagnetism, Kyoto, Nosé, M., Iyemori, T., Sugiura, M., & Kamei, T. (2015). *Geomagnetic Dst index [Dataset].* doi: 10.17593/14515-74000

Wygant, J. R., Bonnell, J. W., Goetz, K., Ergun, R. E., Mozer, F. S., Bale, S. D., ... Tao, J. B. (2013, oct). The electric field and waves instruments on the radiation belt storm probes mission. *Space Science Reviews*, *179*(1-4), 183–220. doi: 10.1007/s11214-013-0013-7

Figure 1.

(a)
(b)
b_r, nT
b_a, nT
$b_{\|}$, nT
E_r, mV/m
E_a, mV/m
f, mHz
UT
L, R_E
04:12
04:24
04:36
04:48
05:00
05:12
04:18
04:30
04:42
04:48
05:06
6.2
6.1

Figure 2.

(a)
06 MLT
L=7
6
5
4
3
2
12
(b)
n, cm^-3
V_A, km/s
UT 2 : 30 3 : 30 4 : 30 5 : 30 6 : 30
L, R_E 5.10 5.91 6.19 6.01 5.40
(c)
V_SW, km/s
n_SW, cm^-3
30
IMF B_z, nT
Dst, nT
AU, AL, nT
UT, h

Figure 3.

(a)
δJ/J
145 keV
110 keV
82 keV
58 keV
38 keV
UT
3:00
3:30
4:00
4:30
5:00
5:30
6:00
6:30
(b)
α, deg
UT
4:12
4:24
4:36
4:48
5:00
5:12
δJ · 10^3, s^-1cm^-2 ster^-1 keV^-1
(c)
CPSD, mV/mHz
38 keV
58 keV
82 keV
f, mHz
(d)
Δφ, deg
ε, keV

Figure 4.

(a)
F, c^3/km^6
0.0003
0.0002
0.0001
Outward
Inward
(b)
$\hat{Q}F/F$, keV^{-1}
1
0.5
0.0
-0.5
-1
UT, hh:mm
L, R_E
03:00 5.6
03:30 5.9
04:00 6.1
04:30 6.2
05:00 6.1
05:30 6.0
06:00 5.8
06:30 5.4
(c)
6
12
0
18
8R$_E$
6
4
2